International Journal of Technical Innovation in Modern Engineering & Science (IJTIMES)
Impact Factor: 3.45 (SJIF-2015), e-ISSN: 2455-2585
Volume 3, Issue 09, September-2017

Improving Performance Of Electric Springs With Current Source Inverter And Fuzzy Logic Controller

R.MONICA[1], P.BHARATH KUMAR[2], P.SUJATHA[3]

[1]Student, Dept. of Electrical and Electronics Engineering, JNTUA, Anantapur, AP, India.

[2]Lecturer, Dept. of Electrical and Electronics Engineering, JNTUA, Anantapur, AP, India.

[3]Professor, Dept. of Electrical and Electronics Engineering, JNTUA, Anantapur, AP, India.

Abstract*— A control technique of direct current control and harmonic distortion work ,similar as the control of active power filter (APF), is proposed utilizing a new kind of electric springs (ESs) with current-source inverters (CSIs) to improve the working of ESs. The total harmonic distortion (THD) can be reduced greatly by changing voltage source inverters (VSIs) to current source inverters (CSIs) and by using fuzzy logic controller. By introducing extra Harmonic Suppression Function (HSF), the System execution can be enhanced further by resolving the input current into fundamental component and other components by using single-stage dq0 technique. Working standards of the proposed ES and control are illustrated.

Index Terms*— Electric spring, direct current control, harmonic suppression, microgrid, renewable energy source.

I. INTRODUCTION

Environment problem has become more severe. With more and more variable renewable power sources the stability of power grid becomes a big issue. The sustainable power sources , for example, wind and sun oriented are relied upon to supplant customary petroleum product [1]. Electric springs (ESs) have been proposed to guarantee the critical loads (CLs) to work in restricted reaches while passing the oscillations to the non-critical loads (NCLs). The underlying idea and the main adaptation of ES are introduced in [2]. The eight compensation capacities is portrayed in [3]. The active suspension idea is embraced in the third form [4], which are joined into bi-directional grid associated converters with no NCLs. Control and equipment execution are portrayed in [5]. The uses of the ESs are illustrated in [6]–[9]. Unity power factor (PF) can be acknowledged by the ESs in [6] and [7]. Active displaying is represented in [10] and [11]. All the ESs examined above are acknowledged by voltage-source inverters (VSIs), none of which comprises of current-source inverters (CSIs). The benefits of CSIs contrasted with VSIs are portrayed in [12]. For example, coordinate current control can be embraced for CSIs. Another control character of CSI is that it acts as a boost inverter [12]–[14]. A few control methods for the ESs are portrayed in [2]–[4].

Two decoupled control loops with corresponding proportional integral (PI) controllers are displayed in [2], one loop of which is intended to manage the CL voltage and another is intended for pure reactive power compensation. As depicted in [9], harmonics might present in such control technique. The δ control displayed in [11] can accomplish two aims together, with just a single parameter δ given to the predefined sinusoidal reference of a corresponding proportional resonant (PR) controller. The viable working ranges of ESs can be identified with δ control to convey the ESs in the circulated control systems. The control targets of the ESs is to balance out the CL voltage, it appears to a learner that it is line impedance that withstands the changes as information voltage fluctuates, than the ES itself. It is difficult to comprehend the ES under voltage control. Performance of electric springs with CSI is described in [15].

This paper presents a control system utilizing new kind of ESs with CSIs and fuzzy logic controller to accomplish a perfect and sinusoidal waveform on CLs.

II. WORKING PRINCIPLES AND CONTROL STRATEGIES OF ESs

The proposed control methodology is to change voltage control to coordinate current control, which needs a controlled current source. In this manner, another ES with CSI is proposed, as appeared in Fig. 1(a), which is regarded as a current controlled current source (CCCS). Other than the distinction in inverter, the huge change in the proposed ES is, a single capacitor C_f utilized as the filter. The present control outline is appeared in Fig. 1(b) where the ES is substituted by a CCCS assigned as i_c and the branch with line impedance is represented by a current source assigned as i_1. Since i_1 varies as v_g changes, the ES needs to generate an ac current to compensate the changes in the input current to accomplish a steady CL voltage. The THD can be reduced by using hysteresis control is shown in Fig. 1(c) which comprises of two practical blocks.

The lower block is comparative as δ control in [11] to accomplish a coveted CL voltage and pure reactive power compensation. It is demonstrated later that THD of CL voltage will be decreased incredibly with this control block. The upper block in Fig. 1(c) originates from the APF, which can help smoother the Total Harmonic components present in the input current to further enhance THD.

III. ANALYSIS OF THE CONTROL METHOD

The direct current control and the detailed design of the control strategy in Figs. 1(b) and (c) are focused in this section. To analyze the concept, the theory of single-phase *dq* transformation should be introduced [16].

A. Control Block with δ Control

In this part, only the control diagrams on the lower side of Figs. 1(c) and (d) are discussed, where the hysteresis controller and PR plus P controllers are used, respectively. As mentioned above, the function of the diagrams are similar as existing δ control and static var generator (SVG). In Fig. 1(c), the signal i_2 is the current through CL. The reference signal i_{2ref} is obtained from δ control. The error signal i_{error} is given to a hysteresis controller where i_{th} is the hysteresis width. The limits of i_H and i_L are compared with the output current of the ES designated as i_c, as shown in Fig. 3(a), to generate four drive signals. With the direct current control in Fig. 1(c), the CL voltage can be regulated to the desired value (e.g. 220V).Also with the reference provided by δ control, the ES can be operated in capacitive, resistive and inductive modes actively as grid voltage varies. A conspicuous favorable advantage is the change on THD which will be checked later.

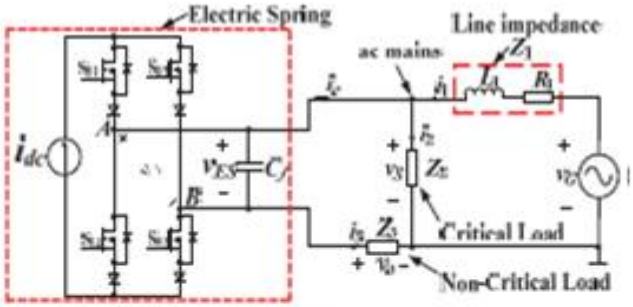

(a)

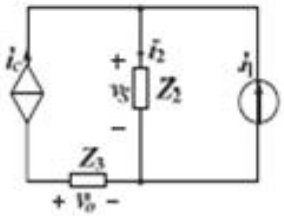

(b)

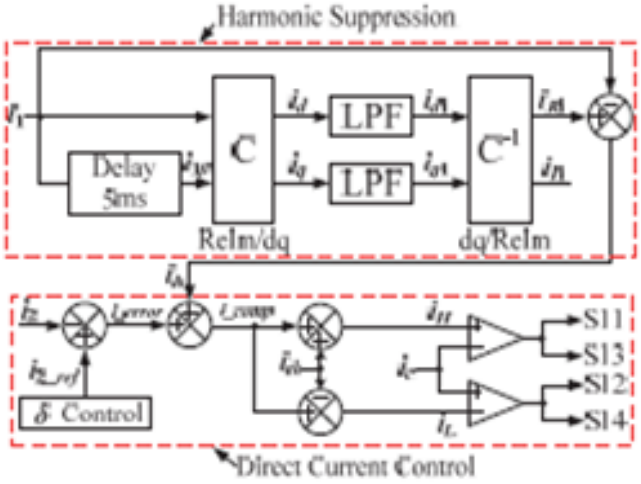

(c)

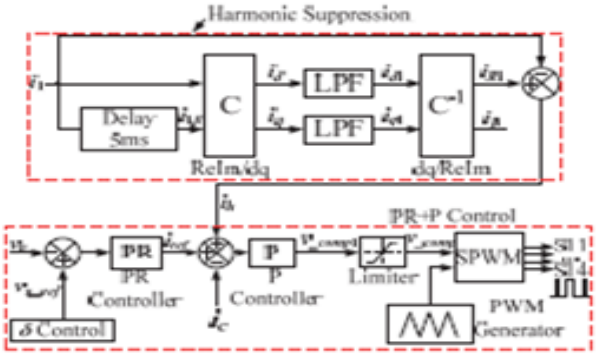

(d)

Fig. 1. Typical application of the ES with CSI and its control. (a) The ES with CSI. (b) Equivalent circuit of (a). (c) The control diagram for hysteresis current control. (d) The control diagram for PR plus P controllers.

Given the high switching frequency of the hysteresis current control, the switching losses and cost ought to be taken in the practical applications. In addition, the CLs should be known to acquire its reference value.Considering these issues, another control methodology with a PR controller, controlling the CL voltage and a P controller, controlling the output current of the ES is proposed in Fig. 1(d).

In the existing δ control, the internal loop controls inductor current and in the proposed control, the internal loop controls the output current of the ES, which is in opposite phase with NCL current.

B. Harmonics Suppression Function and Single-Phase dq Transformation

Harmonic suppression function is presented in the control diagram on the upper side of Figs. 1(c) and (d). In Part A the improvement is seen. Even if the improvement is seen by using direct control but still the THD of CL voltage can be reduced further. In *dq* transformation, the solution is to generate an imaginary signal orthogonal to the measured current. In Fig. 1(c), $i_{1\beta}$ is the fictional signal based on i_1, which is delayed by 5ms. The single-phase *ReIm-to-dq* transformation can be interpreted as follows. Applying Fourier analysis to i_1 gives

$$i_1(t) = i_{1\alpha}(t) = \sum_{n=1}^{\infty} I_n \cos(n\omega_1 t + \varphi_n)$$
$$= I_1 cos\varphi_1 cos\omega_1 t - I_n sin\varphi_1 sin\omega_1 t + \sum_{n=2}^{\infty} I_n \cos(n\omega_1 t + \varphi_n)$$
$$= I_{p1} cos\omega_1 - I_{q1} sin\omega_1 + \sum_{n=2}^{\infty} I_n \cos(n\omega_1 t + \varphi_n) \quad (1)$$

where n is harmonic order, In denotes amplitude of harmonic current at each order, ω_1 is the fundamental angular frequencyφ_n, is the initial phase of harmonic current with respect to the phase of the reference signal. I_{p1} and I_{q1} represent the peak values of active and reactive powers at ω_1 which are expressed as

$$I_{p1} = I_1 cos\varphi_1 \quad (2)$$
$$I_{q1} = I_{q1} sin\omega_1 \quad (3)$$

The fictional signal orthogonal to $i1$ (t) can be expressed as

$$i_{1\beta}(t) = \sum_{n=1}^{\infty} I_n \cos(n\omega_1 t + \varphi_n - \frac{\pi}{2})$$
$$= I_1 cos\varphi_1 cos\omega_1 t + I_n sin\varphi_1 sin\omega_1 t + \sum_{n=2}^{\infty} I_n \sin(n\omega_1 t + \varphi_n)$$
$$= I_{p1} sin\omega_1 + I_{q1} cos\omega_1 + \sum_{n=2}^{\infty} I_n \sin(n\omega_1 t + \varphi_n) \quad (4)$$

Then combine (1) and (4) for the differential form in dq coordinated as

$$\begin{bmatrix} i_d \\ i_q \end{bmatrix} = [C] \begin{bmatrix} i_{1\alpha} \\ i_{1\beta} \end{bmatrix} \quad (5)$$

Where C=$\begin{bmatrix} \cos\theta_0 & \sin\theta_0 \\ -\sin\theta_0 & \cos\theta_0 \end{bmatrix}$, $\theta_0 = \omega_1 t$ is the instantaneous phase angle of the reference signal.

Substituting the matrix C into (5) gives .

$$\begin{bmatrix} i_d \\ i_q \end{bmatrix} = \begin{bmatrix} \cos\theta_0 & \sin\theta_0 \\ -\sin\theta_0 & \cos\theta_0 \end{bmatrix} \begin{bmatrix} i_{1\alpha} \\ i_{1\beta} \end{bmatrix}$$

$$= \begin{bmatrix} i_{1\alpha}\cos\theta_0 & i_{1\beta}\sin\theta_0 \\ -i_{1\alpha}\sin\theta_0 & i_{1\beta}\cos\theta_0 \end{bmatrix} \quad (6)$$

Substituting (1) and (4) into (6) yields

$$\begin{bmatrix} i_d \\ i_q \end{bmatrix} = \begin{bmatrix} I_1 cos\varphi_1 + \sum_{n=2}^{\infty} I_n \cos[(n-1)\omega_1 t + \varphi_n) \\ I_1 sin\varphi_1 + \sum_{n=2}^{\infty} I_n \sin[(n-1)\omega_1 t + \varphi_n) \end{bmatrix} \quad (7)$$

$$= \begin{bmatrix} i_{p1} + \widetilde{I_p} \\ i_{q1} + \widetilde{I_q} \end{bmatrix}$$

Where

$$\widetilde{I_p} = \sum_{n=2}^{\infty} I_n \cos[(n-1)\omega_1 t + \varphi_n \quad (8)$$

$$\widetilde{I_q} = \sum_{n=2}^{\infty} I_n \sin[(n-1)\omega_1 t + \varphi_n \quad (9)$$

$\widetilde{I_p}$ and $\widetilde{I_q}$ are the summation of ac components of all the frequencies in *d* and *q* directions, respectively. It is seen in the *d*-axis that I_{p1} and $\widetilde{I_p}$ represent the dc and ac components, respectively. The same analogy applies to the *q*-axis. If signals at both axes are pure dc components, the results from *dq-to-ReIm* transformation will be the pure sinusoidal signals without any harmonic components. In Fig. 1(c), two low-pass filters (LPFs) are used to make sure i_{d1} and i_{q1} are clean dc components, where

$$I_{d1} = I_{p1} \quad (10)$$

$$I_{q1} = I_{q1} \quad (11)$$

The matrix C^{-1} can be obtained from the matrix C as

$$C^{-1} = \begin{bmatrix} \cos\theta_0 & \sin\theta_0 \\ -\sin\theta_0 & \cos\theta_0 \end{bmatrix} \quad (12)$$

Hence, the *dq-to-ReIm* transformation is as follows.

$$\begin{bmatrix} i_{R1} \\ i_{I1} \end{bmatrix} = [C^{-1}] \begin{bmatrix} i_{d1} \\ i_{q1} \end{bmatrix}$$

$$= \begin{bmatrix} I_1 \cos(\theta_0 + \varphi_1) \\ I_1 \sin(\theta_0 + \varphi_1) \end{bmatrix}$$

$$= \begin{bmatrix} I_1 \cos\varphi_1 cos\omega_1 t - I_1 \sin\varphi_1 sin\omega_1 t \\ I_1 \sin\varphi_1 cos\omega_1 t + I_1 \cos\varphi_1 sin\omega_1 t \end{bmatrix}$$

$$= \begin{bmatrix} \mathrm{Ip1} \cos\omega_1 t - \mathrm{Iq1}\, sin\omega_1 t \\ \mathrm{Iq1} \cos\omega_1 t + \mathrm{Ip1}\, sin\omega_1 t \end{bmatrix} \quad (13)$$

In Fig. 1(c), the summation of harmonic components of input current are defined as

$$i_h = i_1 - i_{R1}$$

Substituting (1) and (13) into (14) yields

$$i_h = \sum_{n=1}^{\infty} I_n \, cos(n\omega_1 t + \varphi_n)$$

The idea is to make, that the harmonic components of input current do not flow into the CL, but to the ES, instead. It will be proved later that THD of the CL voltage with such control strategy are several times less than that only with δ control.

III. FUZZY LOGIC CONTROLLER

The Fuzzy Logic Controller(FLC) is the most popular controller. The basic principle of FLC is the knowledge base which depends upon various if then rules,likely to human operator. Unlike other control strategies, the complex mathematical knowledge is not required.The numbers of rules are 49 for the error and the change in error (inputs of the FLC).

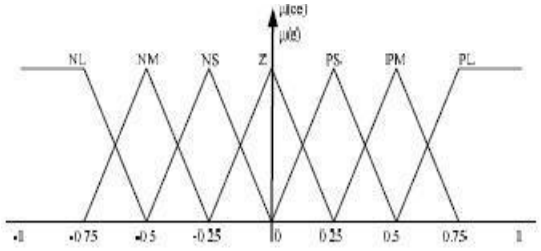

Fig2: Membership functions for error in voltage

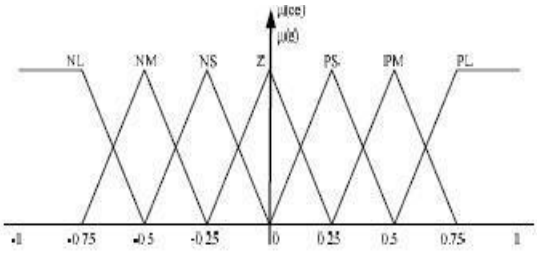

Fig 3:Membership functions for rate of change in error for voltage

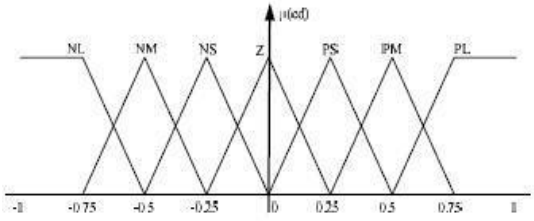

Fig4: Membership functions for output for current

Table I: Rule base of FLC for voltage to current

e/Δe	NL	NM	NS	Z	PS	PM	PL
NL	NL	NL	NL	NL	NM	NS	Z
NM	NL	NL	NL	NM	NS	Z	PS
NS	NL	NL	NM	NS	Z	PS	PM
Z	NL	NM	NS	Z	PS	PM	PL
PS	NM	NS	Z	PS	PM	PL	PL
PM	NS	Z	PS	PM	PL	PL	PL
PL	Z	PS	PM	PL	PL	PL	PL

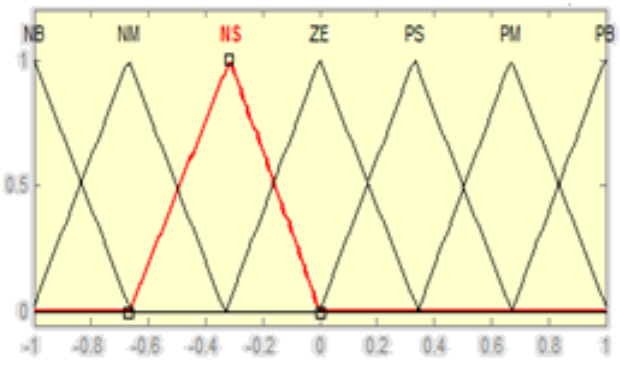

Fig5: membership functions for error in current

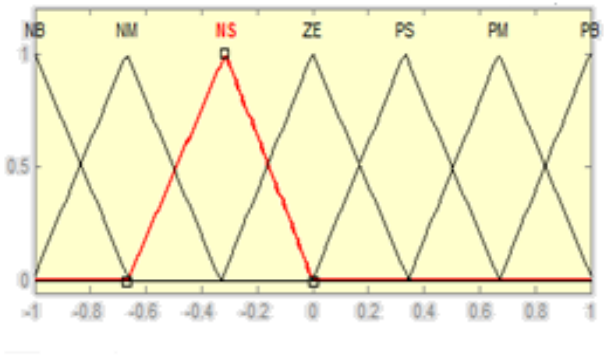

Fig6: Membership function for rate of change in error for current

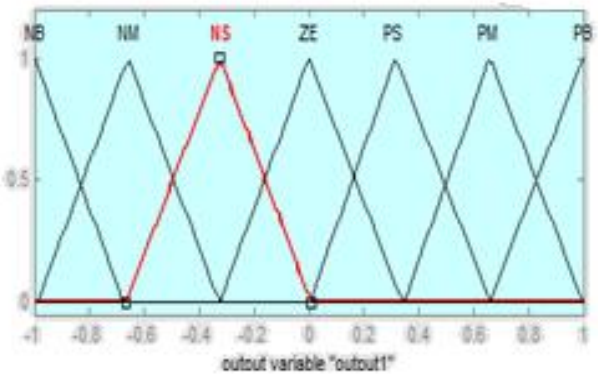

Fig7: membership functions for output voltage

Table II: Rule base of FLC for current to voltage

$e/\Delta e$	NB	NM	NS	ZE	PS	PM	PB
NB	PB	PB	PB	PM	PM	PS	ZE
NM	PB	PB	PM	PM	PS	ZE	ZE
NS	PB	PM	PS	PS	ZE	NM	NB
ZE	PB	PM	PS	ZE	NS	NM	NB
PS	PM	PS	ZE	NS	NM	NB	NB
PM	PS	ZE	NS	NM	NM	NB	NB
PB	ZE	NS	NM	NM	NM	NB	NB

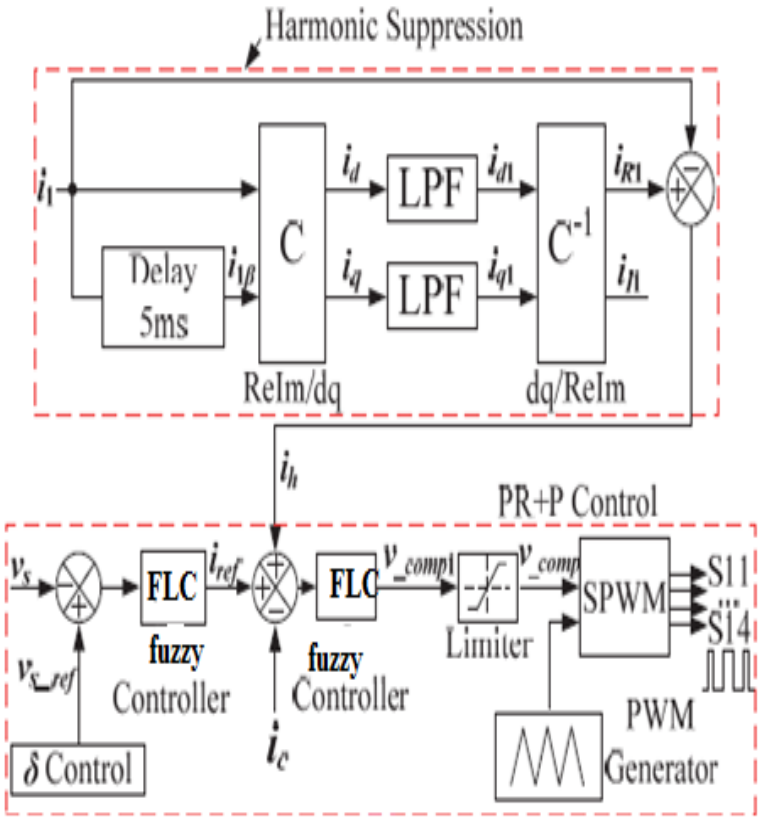

Fig8: ES with CSI controller using fuzzy logic controller

TABLE III

Parameters for simulation

Parameters	values
Reference of critical load voltage (V_S)	220v
Capacitance (C_f)	50μF
Non critical load(R_3)	101.4Ω
Line resistance(R_1)	4Ω
Line inductance (L_1)	84.1mH
Critical load(R_2)	2000Ω
Hysteretic width(i_{th})	0.1A
Cut of frequency of LPF	10HZ

IV.SIMULATION RESULTS

Simulation results using PI controller

Case1: ES with VSI and δ control.

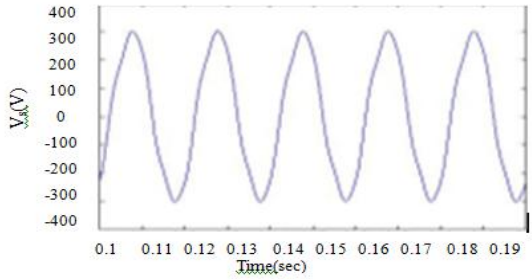

a)Critical Load Voltage

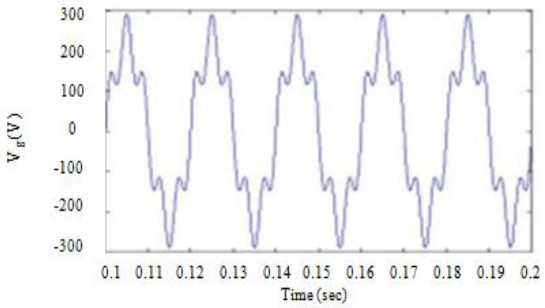

b)Line Voltage with Harmonics

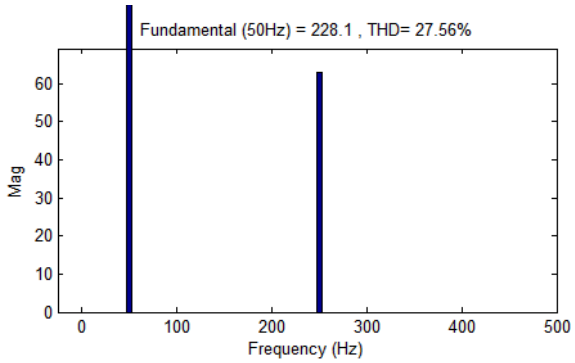

c)FFT analysis of line voltage

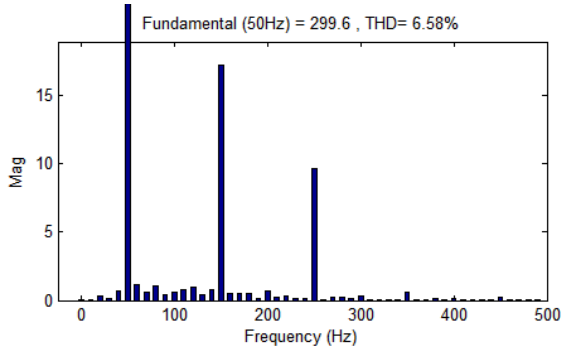

(d) FFT Analysis of critical load voltage.

Fig9: FFT analysis of existing ES with VSI and δ control.

By using VSI the THD of CL voltage is reduced from 27.23% to 6.58%.

Case2: ES with CSI using hysteresis controller

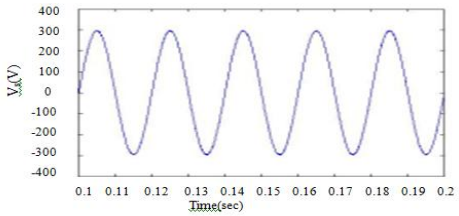

(a) Critical Load Voltage with CSI

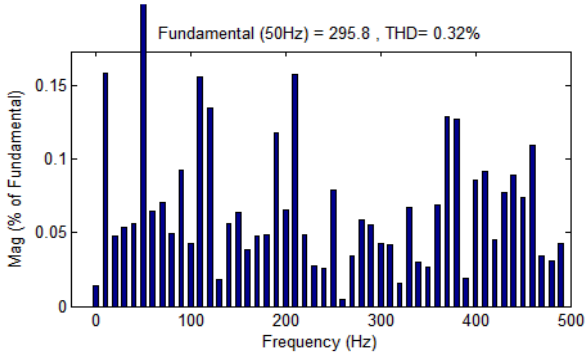

(b) FFT analysis of CL voltage

Fig10: Results of CL voltage with hysteresis controller for an ES with CSI.

The VSI is replaced by CSI and by using hysteresis controller the THD obtained is 0.32%.

Case3: ES with CSI using PR plus P controllers.

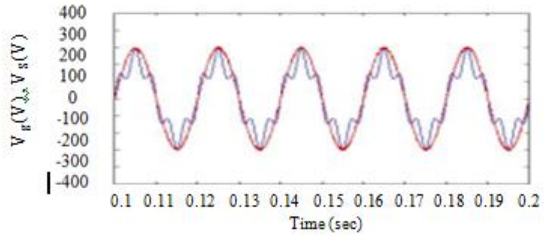

a)Comparison of line voltage and CL voltage

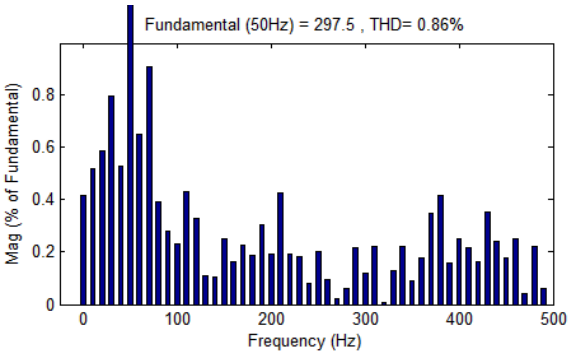

b)FFT analysis of CL voltage

Fig11: Results of input voltage and CL voltage with PR plus P controllers for an ES with CSI.

With PR plus P controller the THD obtained is 0.86%.

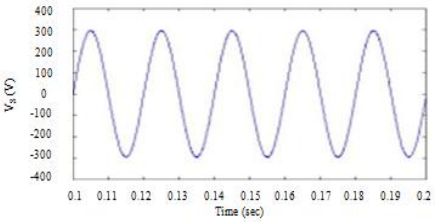

(a) CL Voltage

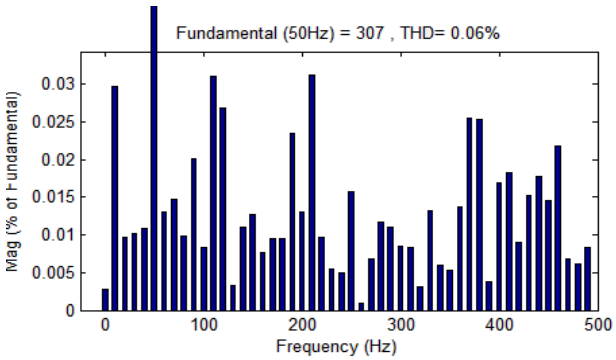

(b)FFT analysis of CL voltage

Fig12: Results of CL voltage with hysteresis controller and APF for an ES with CSI

The THD is reduced to 0.06% by using APF with hysteresis controller.

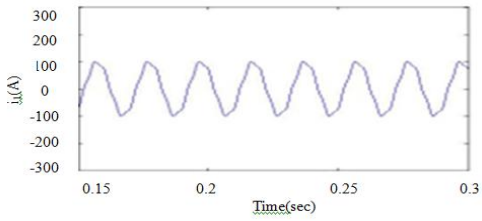

(a) Line Current

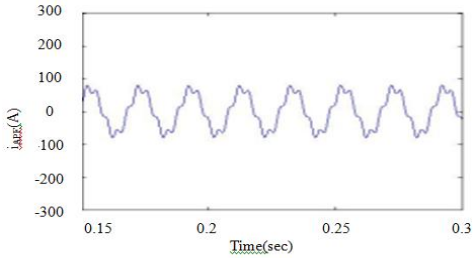

(b) Harmonic Components Of Line Current

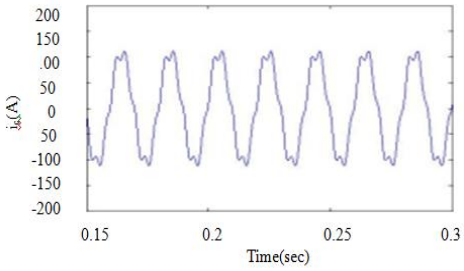

(c) Output Current Of ES

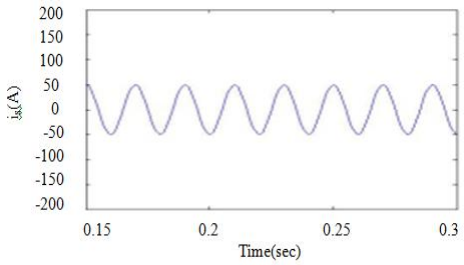

(d) Critical Load Current

Fig13: Current waveforms obtained with harmonic suppression function

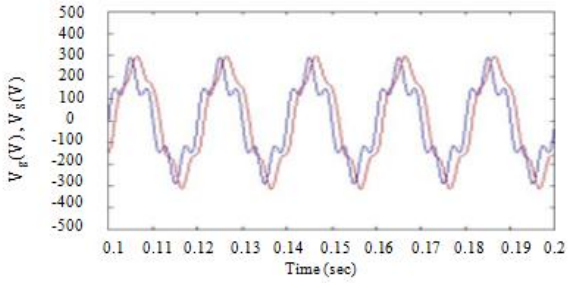

(i) Comparison of line voltage and CL voltage

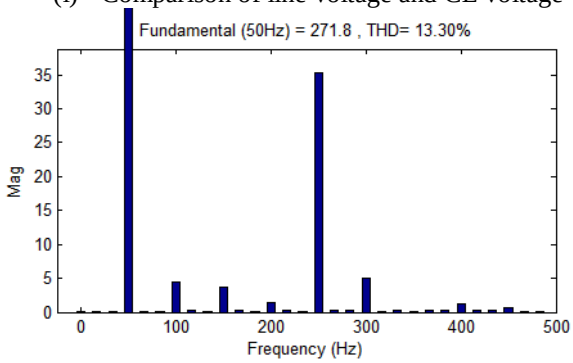

(ii) FFT analysis of CL voltage

(a) without additional harmonics suppressions functions

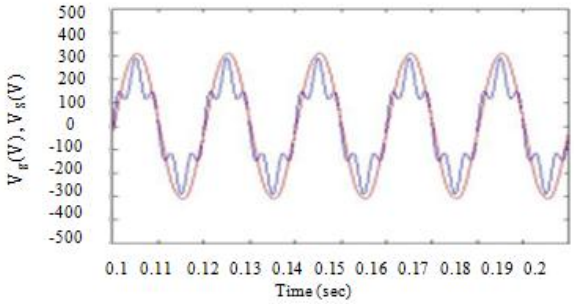

(i) comparison of line voltage and CL voltage

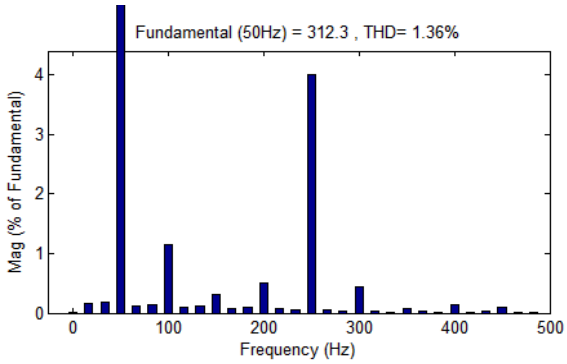

(ii) FFT analysis of CL voltage

(b)With additional harmonics suppression functions

Fig 14: Results using PR plus P controller with and without additional harmonics suppressions function.

By adding harmonic suppression function the THD is decreased and the output waveform can be made more sinusoidal.

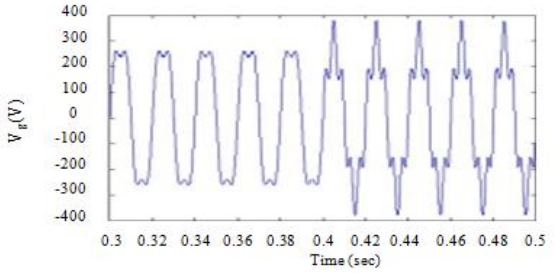

(i) Line Voltage

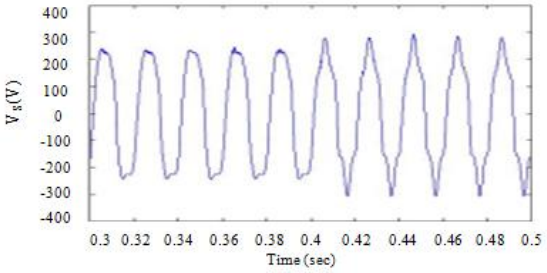

(ii) CL voltage

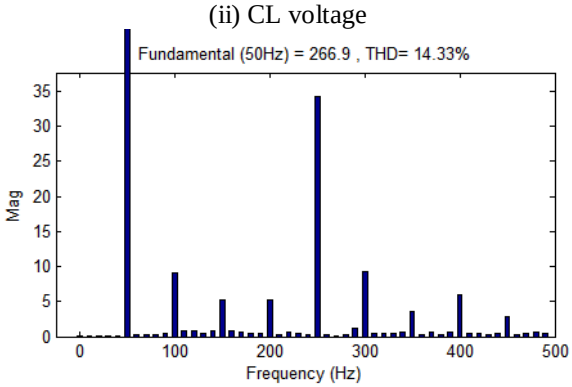

(iii) FFT analysis of CL voltage

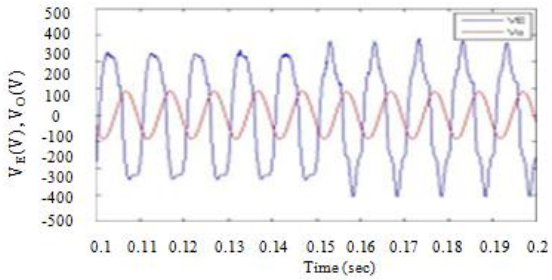

(iv) comparison of voltage across APF and NCL voltage

(a) Without additional harmonics suppressions function

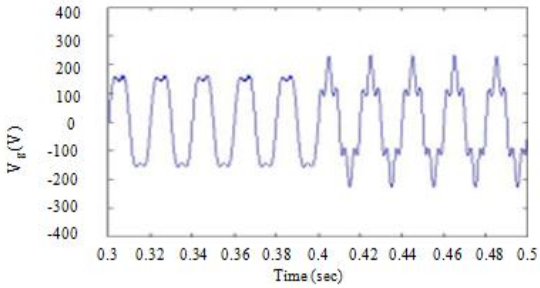

(i) Line Voltage

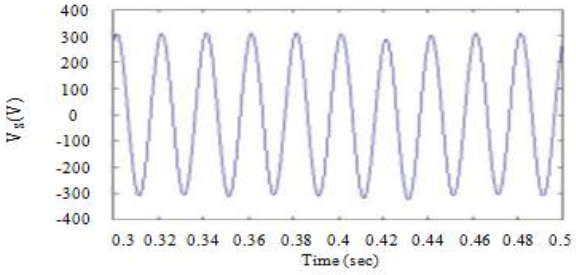

(ii) CL Voltage

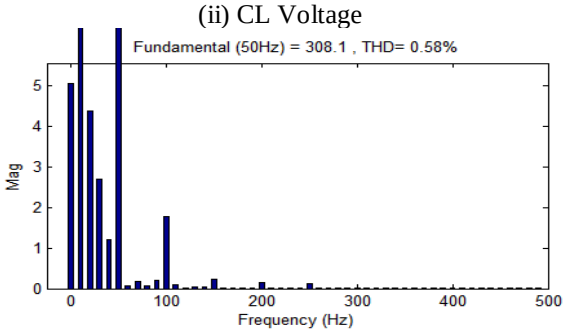

(iii) FFT analysis of CL voltage

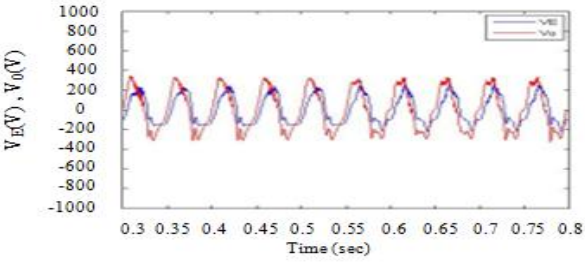

(iv)comparison of voltage across APF and NCL voltage

(b) With additional harmonics suppressions function

Fig 15: Comparison of voltage waveforms with and without additional harmonics suppressions function with different harmonic components

By adding harmonic suppression function the THD is reduced to 0.58%.

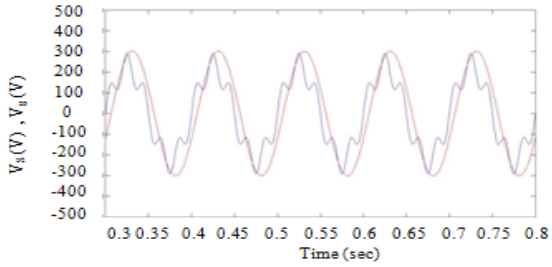

(a) Comparison of line voltage and CL voltage with fuzzy logic controller

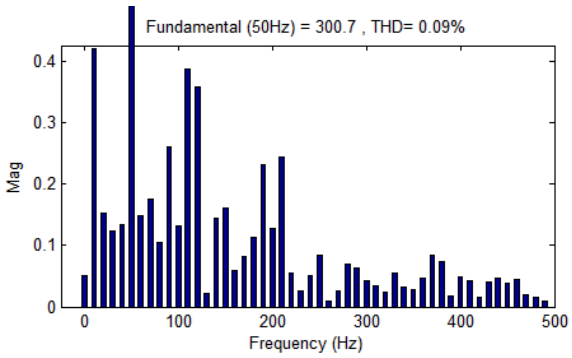

(b) FFT analysis of CL voltage

Fig16: Results of input voltage and CL voltage with fuzzy logic controllers for an ES with CSI.

The Fuzzy Logic Controller replaces the PR plus P controller then the THD is reduced to 0.09%.

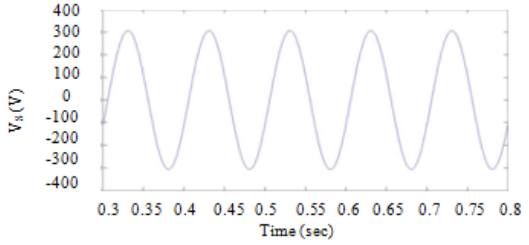

(a) CL Voltage

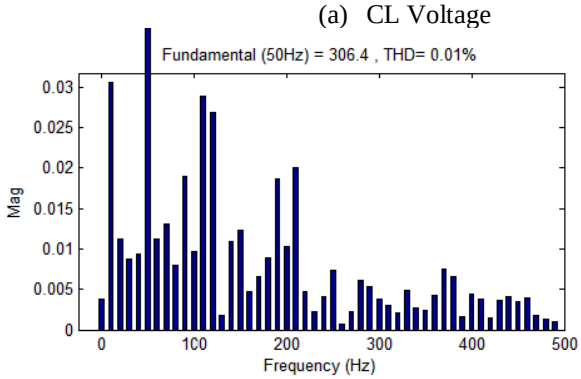

(a) FFT analysis of CL voltage

Fig17: Results of CL voltage with fuzzy logic controllers for an ES with CSI

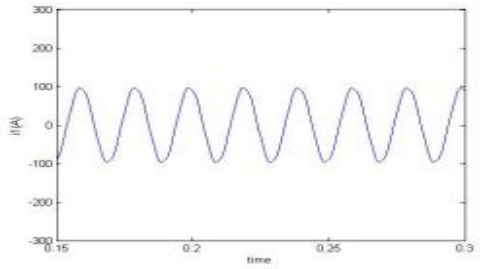

(a) Line Current

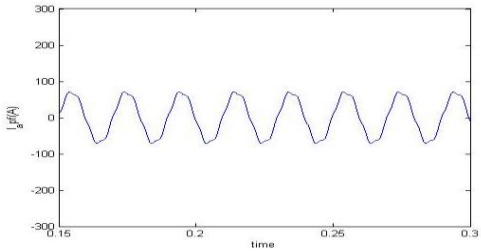

(b) Harmonic Components Of Line Current

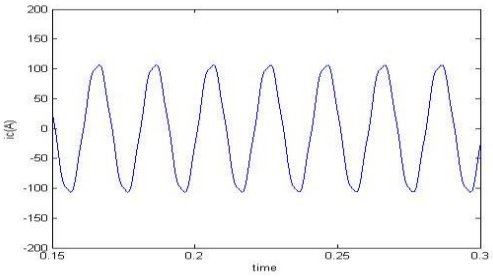

(c) Output Current Of ES

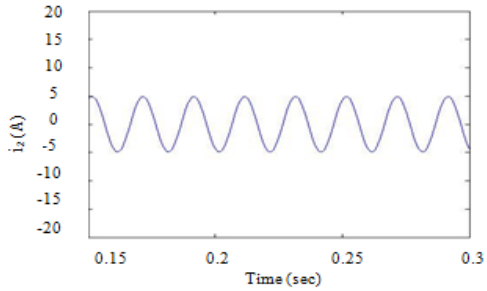

(d) CL Current

Fig18: Current waveforms obtained with fuzzy logic controller

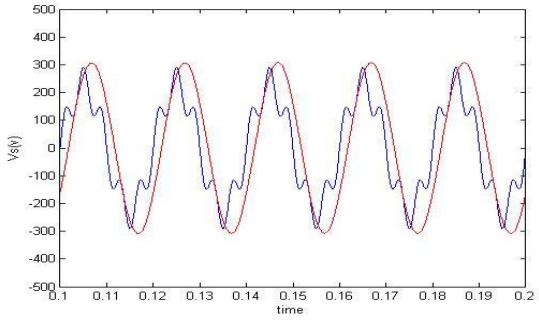

(a) Comparison of line voltage and CL voltage

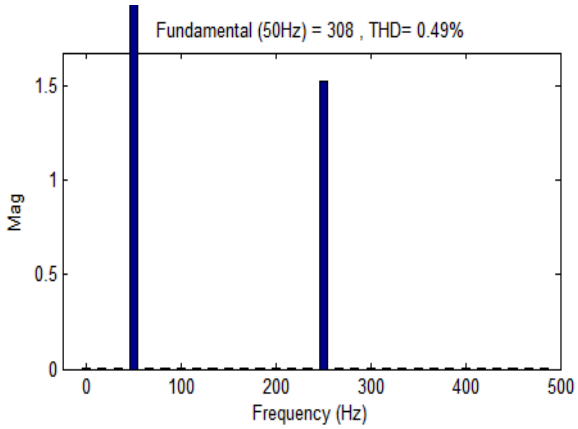

(b) FFT analysis of CL voltage

Fig19: Results using fuzzy controller with additional harmonics suppressions function

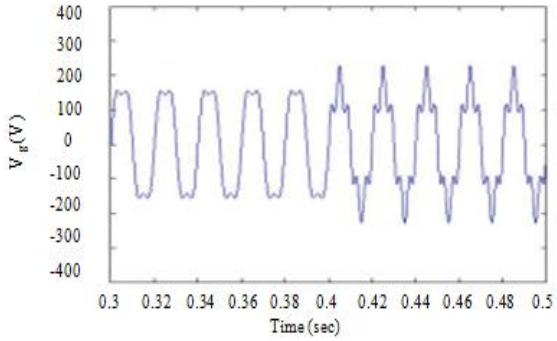

(a) Line Voltage

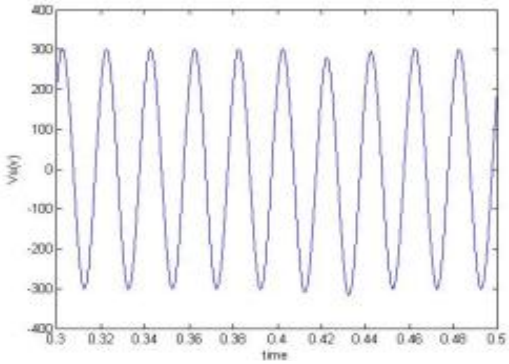

(b) CL voltage

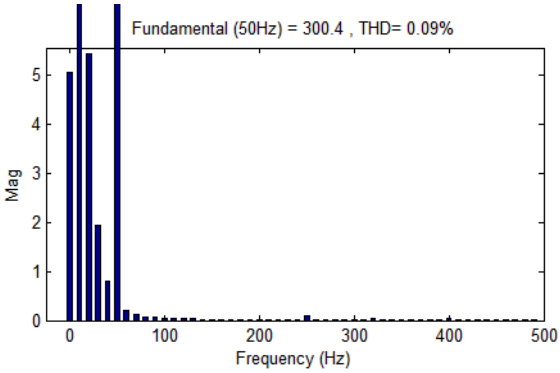

(c) FFT analysis of CL voltage

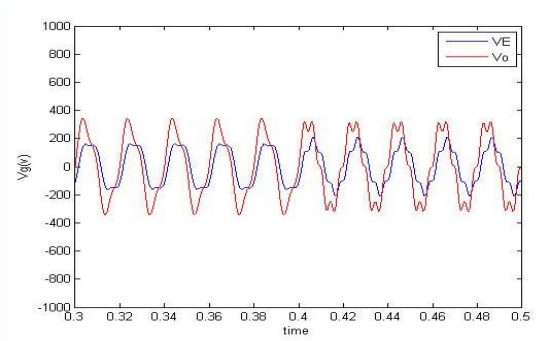

(d)Comparison of voltage across APF and NCL voltage

Fig20: Results when different harmonic components are present using fuzzy controller with additional harmonics suppressions function

TABLE IV

Existing Method	With PI (THD%)	Fuzzy Logic Controller (THD%)
ES with CSI and PR plus P controller	0.86	0.09
ES with APF	0.04	0.01
ES with HSF	1.36	0.49
ES with HSF when different harmonic components are present	0.58	0.09

Where,

APF – Active Power Filter

HSF – Harmonic Suppression Function

VI. Conclusion

A control methodology where existing voltage control on the ES with VSI is replaced by current control on the ES with CSI and fuzzy logic controller is used to decrease the total harmonic distortion. The control method comprise of two blocks, of which one consists the idea of δ control and another is the harmonics suppression function block. The proposed control technique with harmonic suppression function is investigated by using single-stage dq transformation. The control strategies, approving those THD estimations of CL voltage reduce significantly with the proposed coordinate current control than existing voltage control. It is also proved that the harmonic part of CL voltages can further be decreased with the immediate current control and extra harmonic suppression work, particularly valuable for system with high power appraisals.

The fuzzy logic control scheme is designed and implemented in an easier and quicker way than a classical integral control method. Simulation results proved that the fuzzy logic controller performance was better for stabilizing the voltage deviation under different disturbance conditions and also reduce the system ACE comparatively in a short period than the integral controller.

Earlier PR and P controllers are used to control the CL voltage and the output current of ES. In proposed method these controllers are replaced by fuzzy logic controllers. Compared to the existing method the proposed method produced less %THD values.

REFERENCES

[1] M. Cheng and Y. Zhu, "The state of the art of wind energy conversion systems and technologies: A review," Energy Convers. Manag., vol. 88,pp. 332–347, Dec. 2014.
[2] S. Y. R. Hui, C. K. Lee, and F. Wu, "Electric springs—A new smart grid technology," IEEE Trans. Smart Grid, vol. 3, no 3, pp. 1552–1561, Sep;2012.
[3] S. C. Tan, C. K Lee, and S. Y. R. Hui, "General steady-state analysis and control principle of electric springs with active and reactive power compensation," IEEE Trans. Power Electron., vol. 28, no. 8, pp 3958–p. 3969, Aug. 2013.
[4] S. Yan, S. C. Tan, C. K. Lee, B. Chaudhuri and S. Y. R. Hui, "Electric springs for reducing power imbalance in three-phase power systems," IEEE Trans. Power. Electron., vol. 30, no. 7, pp 3601–3609, Jul 2015.
[5] S. Yan, S. C. Tan, C. K. Lee, and S. Y. R. Hui, "Electric spring of power quality improvement," in Proc. IEEE Appl. Power Electron. Conf Expo., 2014, pp. 2140–2147.
[6] C. K. Lee, and S. Y. R. Hui, "Reduction of energy storage requirements in future smart grid using electric springs," IEEE Trans. Smart Grid vol. 4,d, no. 3, pp. 1282–1288, Sep. 2013.
[7] C. K. Lee, B Chaudhuri, and S. Y. R. Hui, "Hardware and control implementation of electric springs for stabilizing future smart grid with intermittent renewable energy sources," IEEE J. Emerging Sel. Topics Power E lectron., vol. 1, no. 1 , pp. 18-27 , Mar 2013.
[8] C. K. Lee, S. C. Tan, F. F. Wu, S. Y. R. Hui and B. Chaudhuri, "Use of Hooke's law for stabilizing future smart grid—the electric spring concept," in Proc. IEEE Energy Convers. Cong Expo., 2013, pp 5253–5257.
[9] Parag Kanjiya, and Vinod Khadkikar, "Enhancing power quality and stability of future smart grid with intermittent renewable energy sources with using electric springs," in Proc IEEE Int. Conf. on Renewable Energy Res. Appl., 2013, pp. 918–922.
[10] N. R. Chaudhuri, C. K. Lee, B Chaudhuri and S. Y. R. Hui, "Dynamic Modeling of Electric Springs," IEEE Trans. Smart Grid, vol. 5, no. 5, pp. 2450–2458, Sep 2014.
[11] Q. Wang, M. Cheng, Z. Chen and Z. Wang,"Steady-state analysis of electric springs with a novel δ control'' IEEE Trans. Power Electron, vol 30,no.12.pp.7159-7169,Dec.2015.
[12]Z. Bai, ,X. Raun and Z. Zhang, "A Generic six-step direct PWM(SS-DPWM) scheme for current source converter," IEEE Trans. Power Electron., vol.25,no.3,pp.3958-3969,Mar.2010.
[13] Y. Chen and K. Smedley, "Three-phase Boost-type grid-connected inverter," IEEE Trans.Power electron., Vol.23, no.5 pp.2301-2309, sep.2008.
[14] N. Zhu, D. Xu, B. Wu, N. R. Zargari, M. Kazerani and F. Liu,"Common-mode voltage reduction methods for current-source converters in medium-voltage drives," IEEE Trans. Power Electron., vol 28, no. 2, pp. 995-1006, Feb. 2013.
[15] Qingsong Wang, Ming Cheng, Yunlei Jiang."Harmonic suppression for critical loads using electric springs with current source inverters," IEEE vol. 4, no. 4, pp. 1362-1369, 2016.
[16] B. Bahrani, A. Rufer, S. Kenzelman, and L.A.C.Lopes,"Vector control of single-phase voltage-source converter based on fictive-axis emulation," IEEE Trans. Ind. Appl., vol. 47, no. 2, pp.831-840, 2011.